Reference power extraction based MPPT technique with enhanced real and reactive power flow control for grid connected DFIG

D.V.N. Ananth[a], G.V. Nagesh Kumar[b*]

[a]Dept. of Electrical & Electronics Engineering, VITAM College of Engineering, Visakhapatnam, India
Tel: +91-8500265310, Email: nagaananth@gmail.com
[b]Dept. of Electrical & Electronics Engineering, GITAM University, Visakhapatnam, India
*Corresponding author: Tel: +91-9000573759, Email:drgvnk14@gmail.com

Abstract

Doubly Fed Induction Generator (DFIG) needs to get adopted to change in wind speeds with sudden change in reactive power or grid terminal voltage as it is required for maintaining synchronism and stability as per modern grid rules. This paper aims to design controller for DFIG converters and MPPT for turbine to maintain equilibrium in rotor speed, generator torque, and stator and rotor voltages and also to meet desired reference real power during the turbulences like sudden change in reactive power or voltage with concurrently changing wind speed. To achieve better power extraction from turbine, maximum power tracking algorithm was designed which changes blade angle and improves the coefficient of power extracted from turbine. To meet desired real power from generator, Rotor Side Controller (RSC) is designed which keeps rotor to rotate at optimal speed and to vary current flow from rotor and stator terminals. Grid Side Converter (GSC) helps in tracking reactive power demand from grid and also helps in maintaining synchronism when grid voltage changes due to fault, at a very faster and stable way. Parameters like tip speed ratio, coefficient of power, stator & rotor voltage, current, real & reactive power, rotor speed and electromagnetic torque are studied using MATLAB simulation. The performance of DFIG is compared when there is wind speed change only, alter in reactive power and variation in grid voltage individually along with variation in wind speed.

Keywords: *Doubly Fed Induction Generator (DFIG), maximum power point tracking (MPPT), real and reactive power control, Rotor & grid side converter (RSC & GSC), wind energy conversion system (WECS)*

NOMENCLATURE

DFIG parameters

L_{ls}, L_{lr}, L_m	Stator or Rotor leakage reactance and magnetizing reactance
R_s, R_r	Stator or Rotor resistance
$V_{sd}, V_{rd}, V_{sq}, V_{rq}$	two axis stator or rotor voltage
$I_{sd}, I_{rd}, I_{sq}, I_{rq}$	two axis stator or rotor current
$\Psi_{sd}, \Psi_{rd}, \Psi_{sq}, \Psi_{rq}$	two axis stator or rotor flux linkage
P_s, P_r	Stator or Rotor real power
Q_s, Q_r	Stator or Rotor reactive power
ω_s, ω_r	Stator or Rotor speed
T_e	Electromagnetic torque
p	Pole pairs
s	Slip
p.u.	per unit

1. Introduction

Wind and solar electric power generation systems are popular renewable energy sources and are getting significance due to retreating of fossil fuels, eco-friendly nature and power availability from few kilo-watts to megawatt [1]. The DFIG is getting importance compared to permanent magnet synchronous generator (PMSG) or asynchronous generator because of its operation under variable speed conditions [3, 5], capability to extract more power using maximum power point tracking theorem (MPPT) [2] fast and accurate control of reactive power [6-13], better capability in low voltage and high voltage fault ride through situation, low cost of converters [14] and effective performance during unbalanced loading and flickering. The efficiency enhancement and capability to meet desired reactive power demand from grid can be obtained by adopting robust RSC for DFIG. But in general, RSC is rated from 25% to 35% of generator stator rating, which allows only ±25% variation in rotor speed [1]. However, due to low power rating of converters, the cost incurred on controllers is low.

In general, the stator and rotor windings of DFIG can deliver both real and reactive power to the grid. The direction of real and reactive power flow from rotor can be varied to meet the desired reactive power requirements from grid with the help of sophisticated RSC controller scheme. The MPPT algorithm will be designed mostly for wind turbines to extract more mechanical power by adjusting the rotor blades and to make the generator shaft to rotate at optimal speed. This algorithm makes the blades to sweep maximum area to make wind sweeping turbine shaft with more mechanical force so that maximum mechanical power can be achieved at that particular wind speed. However more mechanical power can be obtained naturally at higher wind speed from the wind turbine.

The increased penetration of grid connected wind generators leads to many problems for sensitive generators. If some generators among them are, unable to convene desired grid codes, make them to trip, causing decrease in voltage at point of common coupling (PCC) tending the other generators to oscillate following any small disturbance, like change in wind speed. It will tend Wind Energy Conversion System (WECS) to weaken or work at marginal stability for a certain time period. The solution to above penetration issues is effective control of reactive power. To achieve desired reactive power for grid, RSC plays a vital role in coordination with GSC. GSC is necessary to adjust stator voltage, with any change in grid voltage (due to faults etc.), for retaining synchronism with grid and to maintain stability.

Maximum power extraction from DFIG using pitch angle controller and optimal power coefficient at low and high speed is analyzed in [15]. Direct and indirect control of reactive power control with an aim to meet active and reactive power equal to the reference values as achieved in [16]. In this paper, performance of DFIG was compared and analyzed under situations like, with variation in wind speed alone, with reactive power variation and with grid voltage variation for same variation in wind speed. In these cases, variation in tip speed ratio and coefficient of turbine power, effect on real and reactive power flows, voltages and current from stator and rotor, rotor speed and electromagnetic torque are examined. The paper has been organized with overview of WECS with wind turbine modeling and pitch angle controller in 2nd section, study of mathematical modeling of DFIG in 3rd section, the 4th section describe RSC architecture and design; section 5 analyses the performance of DFIG for three cases namely effect of variation on wind speed variation, reactive power demand along with variation in wind speed and grid voltage variation with wind speed. Section 6 presents conclusion and system parameters have been given in appendix.

2. Wind energy conversion system (WECS)

The overview of wind energy conversion system (WECS) is shown in Fig. 1. The construction has following dynamic models: Wind speed calculator is an anemometer sensor system with storage system to measure the actual wind speed in meters per second at that instant with air density and ambient temperature measurements also, and is given to WECS and turbine system. The WECS system consists of aerodynamics and wind turbine control model to extract maximum power during steady state and protection during transient or unstable state of operation. Mechanical and electrical model control system is to generate reference speed, power and voltage signals for controlling real and reactive power flow from generator to the grid and also contains protective system during

abnormal situation. The mechanical model system gives command to turbine for extraction of maximum mechanical power extraction for a given wind speed and the electrical model system give command for the generator to produce respective real power and reactive power and to maintain synchronism under all operating condition.

The real and reactive power from DFIG is controlled by using two controllers namely RSC and GSC using converter controller model as shown in Fig.2. The converter model is bidirectional switches with IGBT (integrated bi-polar transistor), which controls the voltage, real and reactive power from stator and rotor to grid.
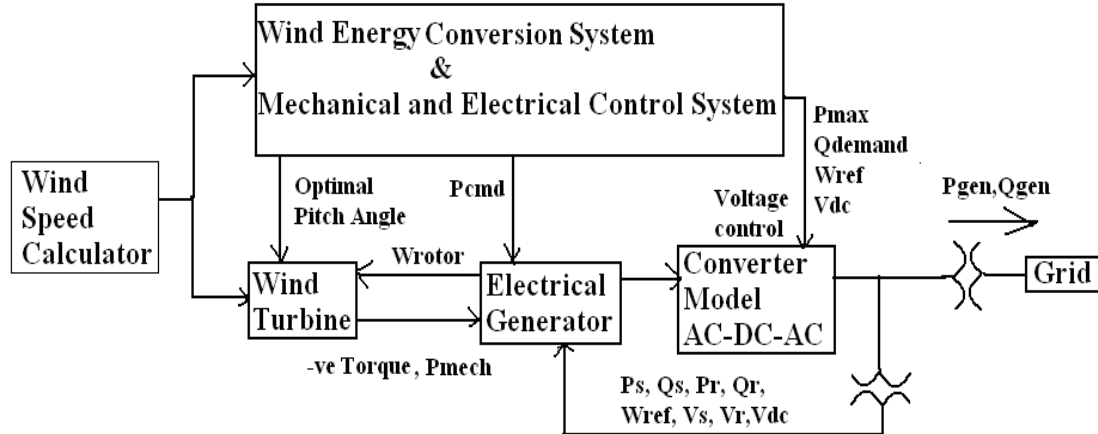

Figure 1 Block diagram of WECS for grid connected DFIG

The RSC aim is to maintain DFIG rotor to maintain optimal speed specified by MPPT and also to control the reactive power flow by varying rotor current direction. The GSC maintains constant DC link voltage at back to back terminals across capacitor, so that this voltage can be maintained as per PCC and also for rapid supply of leading or lagging reactive power without much deviation from generator real power.

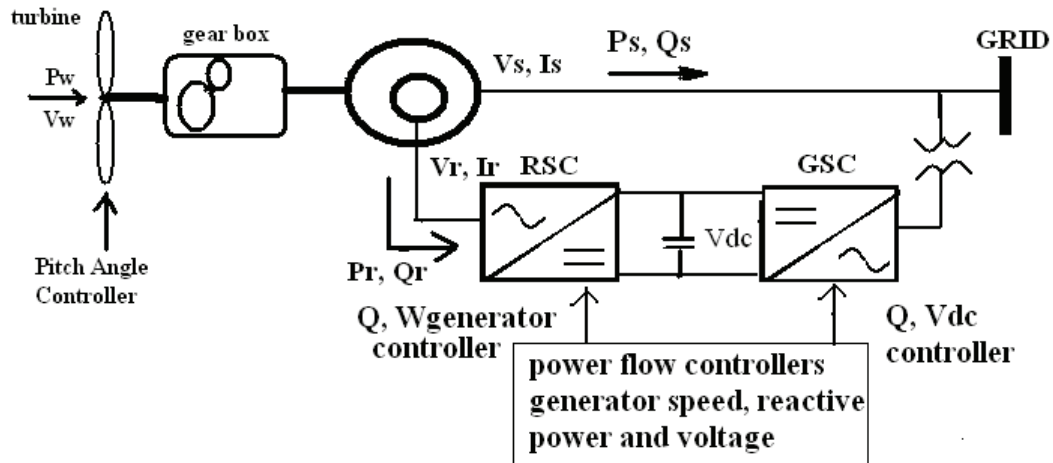The transformer near the grid is step-up type and the other transformer is an isolation transformer.

Figure 2 Schematic diagram of WECS for DFIG system connected to grid

2.1 The wind turbine modeling

The wind turbine is the prime mover which facilitates in converting kinetic energy of wind into mechanical energy which further transforms into electrical energy using a generator. From basic theory of wind energy conversion, the output mechanical power from turbine is given by

$$P_{mech} = \frac{1}{2}C_p(\lambda, \beta)\rho\pi r^2 v_\omega^3 \qquad (1)$$

Where P_{mech} is the mechanical power output from wind turbine, C_p is coefficient of wind power as a function of pitch angle (β) and tip speed ratio (λ), ρ is specific density of air, r is radius of wind turbine blade, v_ω is wind speed.

$$C_p(\lambda, \beta) = 0.5176 \left(\frac{116}{\lambda_i} - 0.4\,\beta - 5\right) e^{-21/\lambda_i} + 0.0068\lambda \qquad (2)$$

The tip sped ratio is a relation between turbine speed (ω_t), radius of turbine blades and wind speed and tip speed ratio at particular angle 'i' is given the relation as shown below

$$\lambda = \frac{\omega_t r}{v_\omega} \quad and \quad \frac{1}{\lambda_i} = \frac{1}{\lambda + 0.08\beta} - \frac{0.035}{\beta^3 + 1} \qquad (3)$$

the output power at nominal wind speed is given by the below equation

$$v_n = \sqrt[3]{\frac{2\,P_{sh}}{\pi\rho r^3 C_{p\,max}}} \qquad (4)$$

Where P_{sh} is the turbine shaft power and C_{pmax} is maximum mechanical power coefficient. The maximum power P_{max} from wind turbine can be extracted by using the equation

$$P_{max} = \frac{1}{2\lambda_{opt}^3}\pi\rho C_{p\,max} r^5 \omega_{opt}^3 \qquad (5)$$

2.2 Pitch angle controller

The wind turbine blade angles are controlled by using servo mechanism to maximize turbine output mechanical power during steady state and to protect the turbine during high wind speeds.

This control mechanism is known as pitch angle controller. When wind speed is at cut-in speed, the blade pitch angle is set to produce optimal power, at rated wind speed; it is set to produce rated output power from generator. At higher wind speeds, this angle increases and makes the turbine to protect from over-speeding. The pitch angle controller circuit is as shown in Fig. 3.
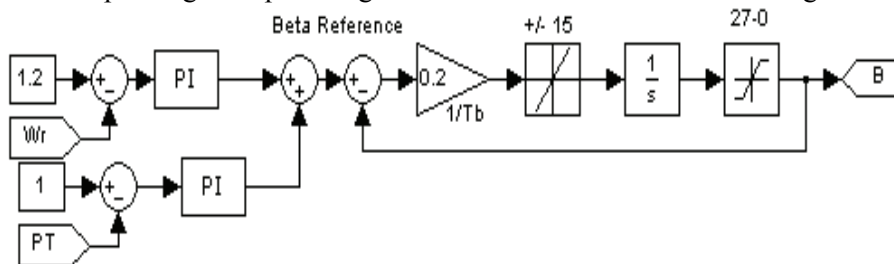

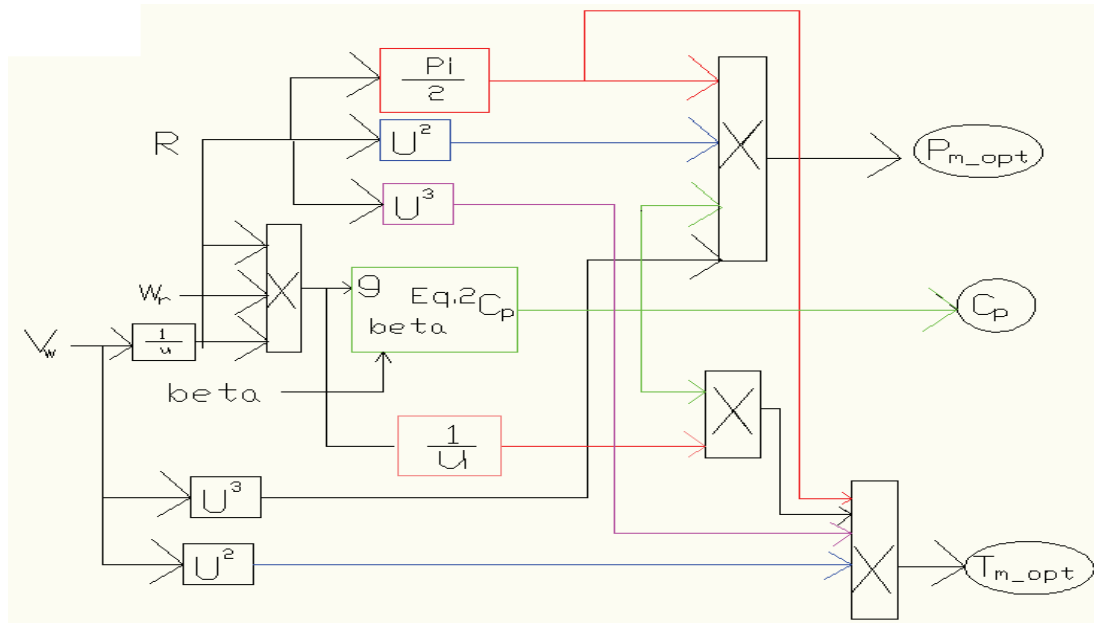Figure 3 Pitch angle controller design for wind turbine

Figure 4 Reference electrical power generation control circuit and mechanical torque output from turbine with MPPT algorithm

In this system reference generator speed is W_r^{ref} =1.2p.u and actual speed of the generator is Wr. The error between reference and actual values is controlled using PI controller. In the similar way, the difference in reference (P*=1) and actual power outputs from turbine (PT) is controlled by PI controller. Both the outputs from PI controller are designed to get reference pitch angle controller (β_{ref}). The closed loop control of pitch angle is obtained as shown in Fig.3. The optimal pitch angle is written mathematically at this point as $\int \frac{1}{T_\beta}(\beta_{ref} - \beta)\, dt$. If pitch angle is set at zero degrees, maximum power can be extracted from the turbine. In general pitch angle is set between 0° to 7.5° per second to extract maximum power, also these values specify that the turbine is working in stable environment and if is set at 27° per second, it means either wind speed is high called cutout wind speed or may be external fault in the external electric system has occurred. The reference real power (P_e) or actual mechanical output from turbine and mechanical output torque (T_m) is shown in Fig.4. Using Tip Speed Ratio (TSR) and Coefficient of Power (C_P) to generate reference power and the control scheme is useful to extract maximum mechanical power, thereby more mechanical torque T_m by using the MPPT algorithm.

The aim of MPPT algorithm as shown in Fig. 4 is to generate optimal mechanical power output from turbine and mechanical input torque to be given to the doubly fed induction generator. The mechanical power is given as reference to GSC to make the rotor to rotate at optimal speed. The optimal input torque to DFIG is so as to operate for extracting maximum power from the generator. The inputs to MPPT algorithm are radius of curvature (R) of turbine wings, rotor speed (W_r), wind speed (V_w) and pitch angle (beta). Initially with R, W_r and V_w, tip speed ratio (g) is determined. Later using equation 2 and input parameter beta, coefficient of power (C_p) is calculated. Based on equation 5, optimal mechanical power (P_{m_opt}) is determined and dividing mechanical power by rotor speed, optimal torque (T_{m_opt}) is determined. The pitch angle (beta) is determined as shown in Fig.4. The application of P_{m_opt} and T_{m_opt} is shown in Fig. 6 and 7.

When there is change in wind speed, turbine speed changes and thereby beta, C_p and mechanical power and torque changes [2]. If grid voltage varies due to fault or any conditions, the current flow in the rotor circuit varies. Huge requirement of reactive power for grid will come to picture to maintain low voltage ride through (LVRT) phenomenon. During this period, rotor speed increases gradually and loose synchronism if not provided with LVRT capability [14]. In general, load varies continuously. So, active and reactive power demand from grid changes considerably. It has to be provided by DFIG. For this enhanced real and reactive power is necessary [12]. For this, optimal real power generation is achieved by extracting optimal mechanical power output from turbine is derived

and made to run at optimal loading and speed. For this MPPT algorithm proposed will be very helpful.

2.3 Mathematical Modeling of DFIG

There are many advantages of DFIG compared to squirrel cage induction generator or permanent magnet synchronous generator. Using DFIG independent control of active and reactive power, variable speed and constant frequency operation, over load capability, higher efficiency, higher ratings, are possible. The converters need to handle only 25% to 35% of generator capacity, thereby minimizing operating cost & switching losses and low hardware cost etc.

The equivalent circuit of DFIG in rotating reference frame at an arbitrary reference speed of ω is shown in Fig. 5. The equations can be derived in dq reference frame as follows:
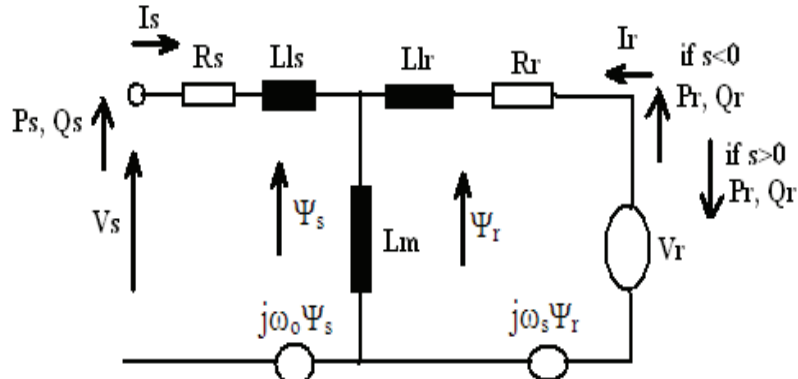

Figure 5 Equivalent circuit of DFIG in rotating reference frame at speed ω

The stator direct and quadrature axis (dq) voltages of DFIG can be written as

$$V_{sd} = R_s I_{sd} - \omega_s \psi_{sq} + \frac{d\psi_{sd}}{dt} \tag{6}$$

$$V_{sq} = R_s I_{sq} + \omega_s \psi_{sd} + \frac{d\psi_{sq}}{dt} \tag{7}$$

The rotor direct and quadrature axis voltages have been derived as

$$V_{rd} = R_r I_{rd} - (\omega_s - \omega_r)\psi_{rq} + \frac{d\psi_{rd}}{dt} \tag{8}$$

$$V_{rq} = R_r I_{rq} + (\omega_s - \omega_r)\psi_{rd} + \frac{d\psi_{rq}}{dt} \tag{9}$$

The difference between stator speed (ω_s) and rotor speed (ω_r) is known as slip speed ($s\omega_s$). For motoring action, this difference is less than zero and for generating, the slip speed is negative. The stator and rotor flux linkages in axis frame are given below

$$\psi_{sd} = L_{ls} I_{sd} + L_m I_{rd} \tag{10}$$

$$or\ \psi_{sd} = L_m I_{sm} \tag{11}$$

$$\psi_{sq} = L_{ls} I_{sq} + L_m I_{rq} \tag{12}$$

$$\psi_{rd} = L_{lr} I_{rd} + L_m I_{sd} \tag{13}$$

$$\psi_{rq} = L_{lr} I_{rq} + L_m I_{sq} \tag{14}$$

The stator real power in terms of two axis voltage and current is

$$P_s = \frac{3}{2}(V_{sd} I_{sd} + V_{sq} I_{sq}) \tag{15}$$

The rotor real power in terms of two axis voltage and current is

$$P_r = \frac{3}{2} \left(V_{rd} I_{rd} + V_{rq} I_{rq} \right) \tag{16}$$

The stator reactive power in terms of two axis voltage and current is

$$Q_s = \frac{3}{2} \left(V_{sq} I_{sd} - V_{sd} I_{sq} \right) \tag{17}$$

The rotor reactive power in terms of two axis voltage and current is

$$Q_r = \frac{3}{2} \left(V_{rq} I_{rd} - V_{rd} I_{rq} \right) \tag{18}$$

The quadrature and direct axis rotor current in terms of stator parameters can be written as

$$I_{rq} = \frac{P_s}{|V_s|} = \frac{-L_{ls}}{L_m} I_{sq} \tag{19}$$

$$I_{rd} = \frac{Q_s}{|V_s|} + \frac{|V_s|}{\omega_s L_m} \tag{20}$$

The output electromagnetic torque is given by the equation

$$T_e = \frac{3}{2} L_m \left(I_{sq} I_{rd} - I_{sd} I_{rq} \right) \tag{21}$$

The mechanical torque output from the turbine in terms of mechanical power and rotor speed is

$$T_m = \frac{P_{mech}}{\omega_r} \tag{22}$$

3. Rotor side controller (RSC) and Grid side controller (GSC) architecture and design

3.1 Operation of GSC and RSC

The RSC is used to control the speed of rotor and also helps in maintaining desired grid voltage. The control circuit for GSC is shown in Fig. 6 and RSC is shown in Fig. 7 with internal circuits for deriving RSC PLL for 2 phases to 3 phases inverse Parks transformation is shown in Fig. 8. This Fig.8 helps to inject current in rotor winding at slip frequency. The GSC and RSC have four control loops each, later has one speed control loop, other is reactive power and last two are direct and quadrature axis current control loops. The speed and reactive power control loops are called outer control loop and direct and quadrature axis control loops are called inner control loops. The reference rotor speed is derived from the wind turbine optimal power output $P_m{}^{Opt}$ as shown in Fig.4 and grid power demand. In total, the reference power input to the lookup table as shown in Fig.7 is $P_{m,g}{}^{Opt}$. Based on the value of $P_{m,g}{}^{Opt}$, the rotor is made to rotate at optimal speed so as to extract maximum power from DFIG set. The difference between reference speed of generator and actual speed of generator is said to be rotor speed error. Speed error is minimized and maintained nearly at zero value by using speed controller loop which is a PI controller with K_{pn} and K_{in} as proportional and integral gain parameters. The output from speed controller is multiplied with stator flux (F_s) and ratio of stator and rotor (L_s and L_r) inductances to get reference quadrature current (I_{qr}) for rotor. The error in reference and actual reactive power give reference direct axis current (I_{qr}). The difference between these reference and actual two axis currents is controlled by tuned PI controller to get respective direct and quadrature axis voltages. The output from each PI controller is manipulated with disturbance voltages to get reference voltage for pulse generation as shown in Fig. 7. It must be noted that the pulses are regulated at slip frequency for RSC rather than at fundamental frequency and slip frequency synchronizing for inverse Park's transformation can also be seen in the figure.

The MATLAB based block diagram of GSC is shown in Fig. 6. For a given wind speed, reference or control power from turbine is estimated using lookup table. From equation (15), stator real power (P_{stator}) is calculated and the error in powers is difference between these two powers (dP) which is to be maintained near zero by PI controller. The output from PI controller is multiplied with real power constant (K_p) gives actual controllable power after disturbance. The difference in square of

reference voltage across capacitor dc link (V_{dc}^*) and square of actual dc link voltage (V_{dc}) is controlled using PI controller to get reference controllable real power. The error in the reference and actual controllable power is divided by using 2/3Vsd to get direct axis (d-axis) reference current near grid terminal (I_{gdref}). Difference in I_{gdref} and actual d-axis grid current is controlled by PI controller to get d-axis voltage. But to achieve better response during transient conditions, decoupling d-axis voltage is added as in case of separately excited DC motor. This decoupling term helps in controlling steady state error and fastens transient response of DFIG during low voltage ride through (LVRT) or during sudden changes in real or reactive powers from/ to the system.

   Similarly from stator RMS voltage (Vs) or reference reactive power, actual stator voltage or reactive power is subtracted by PI controller and multiplied with appropriate reactive power constant (K_q) to get actual reference reactive power compensating parameter. From equation (17), actual reactive power is calculated and the difference in this and actual compensating reactive power and when divided by 2/3Vsq, we get quadrature axis (q-axis) reference current (I_{qref}). When the difference in I_{qref} and stator actual q-axis current (I_q) is controlled by PI controller, reference q-axis voltage is obtained. As said earlier, to improve transient response and to control steady state error, decoupled q-axis voltage has to be added as shown in Fig. 6. Both d and q axis voltage parameters so obtained are converted to three axis abc parameters by using inverse Park's transformation and reference voltage is given to scalar PWM controller to get pulses for grid side controller.

   The main purpose of rotor side controller (RSC) is to maintain desired generator speed and reactive power flow from rotor circuit, while grid side controller (GSC) is used to achieve nearly constant DC link voltage and to control bidirectional reactive power flow from GSC converter, stator and grid. This GSC is also capable of controlling real power from stator to achieve desired real power from generator stator.
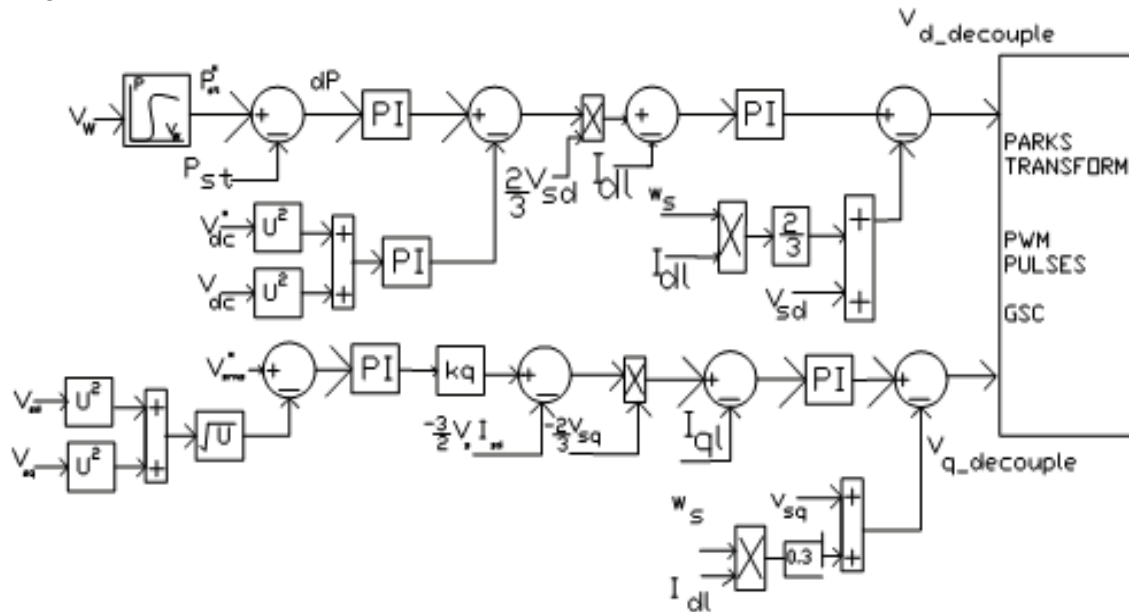

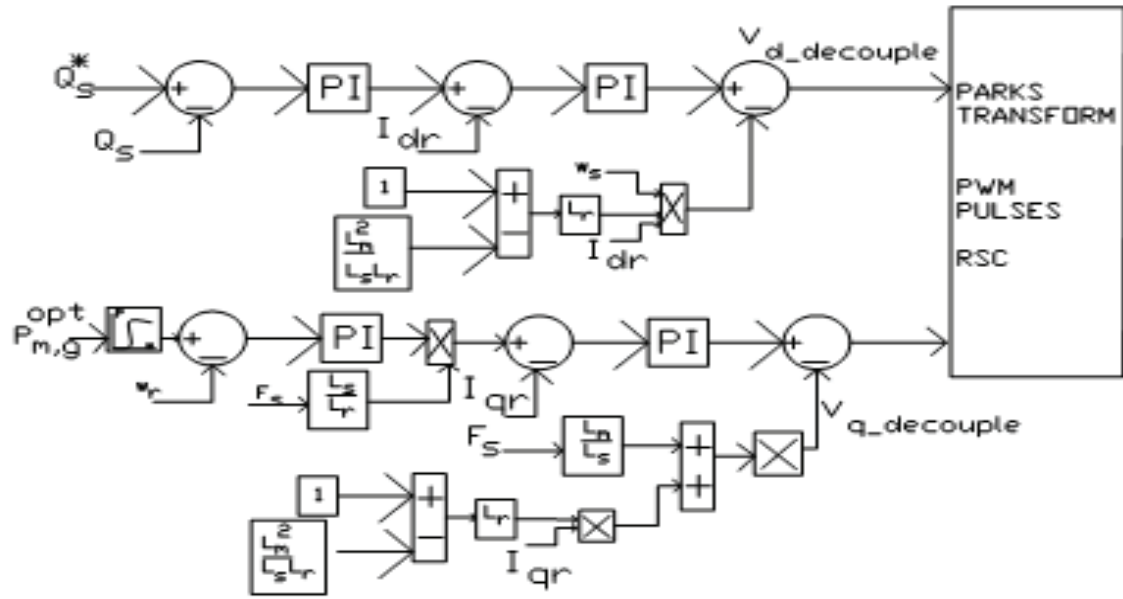Figure 6 Grid side controller for DFIG
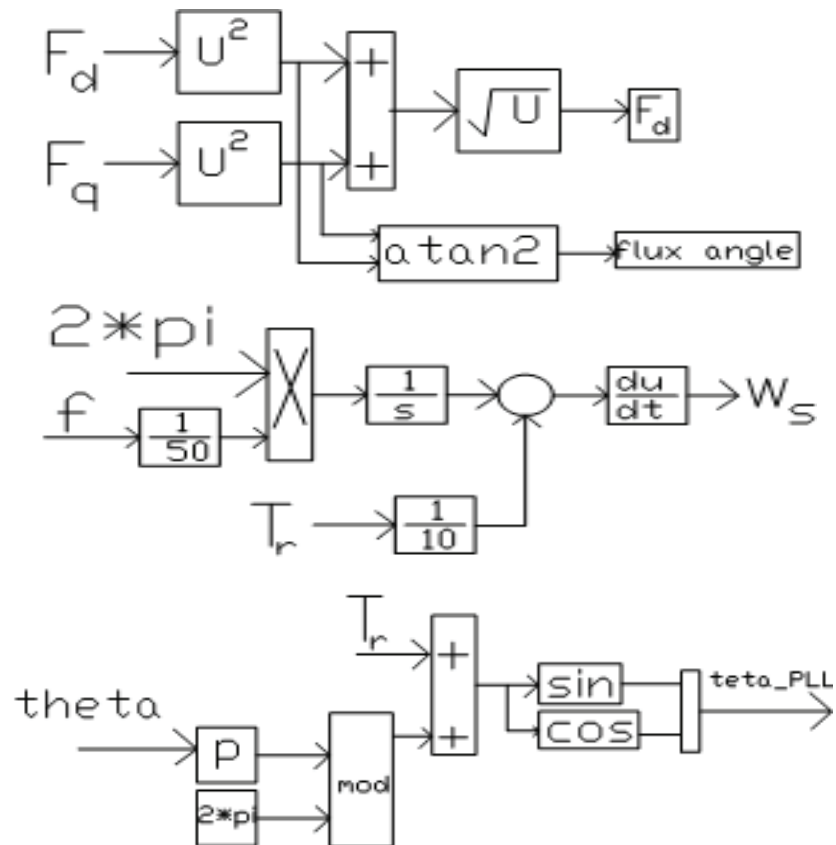
Figure 7 Rotor side controller for DFIG

Figure 8 Internal circuits design of RSC for extracting rotor Parks transform PLL block for dq to abc conversion

The general form of speed regulation is given by

$$T_e = J\frac{d\omega_r}{dt} + B\,\omega_r + T_l \tag{23a}$$

$$= (Js+B)\,\omega_r + T_l \tag{23b}$$

Where T_e is electromagnetic torque, J is moment of inertia and B is friction coefficient, T_l is considered to be disturbance.

Multiplying both sides with ω_{error} , we get the equation as

$$T_e \, \omega_{error} = (Js + B) \, \omega_r \, \omega_{error} + T_l \, \omega_{error} \tag{24}$$

Considering ω_r constant and change in speed error is ω_{error} is control variable, the above equation becomes.

$$P_s^* = (K_{in}s + K_{pn}) \, \omega_{error} + P_l \tag{25}$$

As product of torque and speed is power, we will be getting stator reference power and disturbance power as shown below.

$$P_s^* - P_l = (K_{in}s + K_{pn}) \, \omega_{error} \tag{26}$$

Where, $K_{in} = J*\omega_r$ and $K_{pn} = B*\omega_r$

Finally direct axis reference voltage can be written by using equation (26) and from Fig. 6 is

$$V_{rd}^* = -(\omega_{error})(K_{pn} + \frac{K_{in}}{s}) + (P_s)(K_{pt} + \frac{K_{it}}{s}) \tag{27}$$

$$V_{rq}^* = Q_{error} (K_{pQ} + \frac{K_{iQ}}{s}) \tag{28}$$

$$V_{gd}^* = K_{gp}(i_{gd}^* - i_{gd}) + k_{gi} \int (i_{gd}^* - i_{gd})dt - \omega_o L_g i_{gd} + +k_1 V_{sd} \tag{29}$$

$$V_{gq}^* = K_{gp}(i_{gq}^* - i_{gq}) + k_{gi} \int (i_{gq}^* - i_{gq})dt + \omega_o L_g i_{gd} + k_2 V_{sq} \tag{30}$$

$$i_{gq}^* = K_q sqrt(V_{dc}^{2*} - V_{dc}^2) + k_{qi} \int (V_{dc}^* - V_{dc})dt + R_{dc}V_{dc} \tag{31}$$

$$i_{gd}^* = K_d sqrt(V_s^{2*} - V_s^2) + k_{di} \int (V_s^* - V_s)dt \tag{32}$$

The rotating direct and quadrature reference voltages of rotor are converted into stationary abc frame parameters by using inverse parks transformation. Slip frequency is used to generate sinusoidal and cosine parameters for inverse parks transformation.
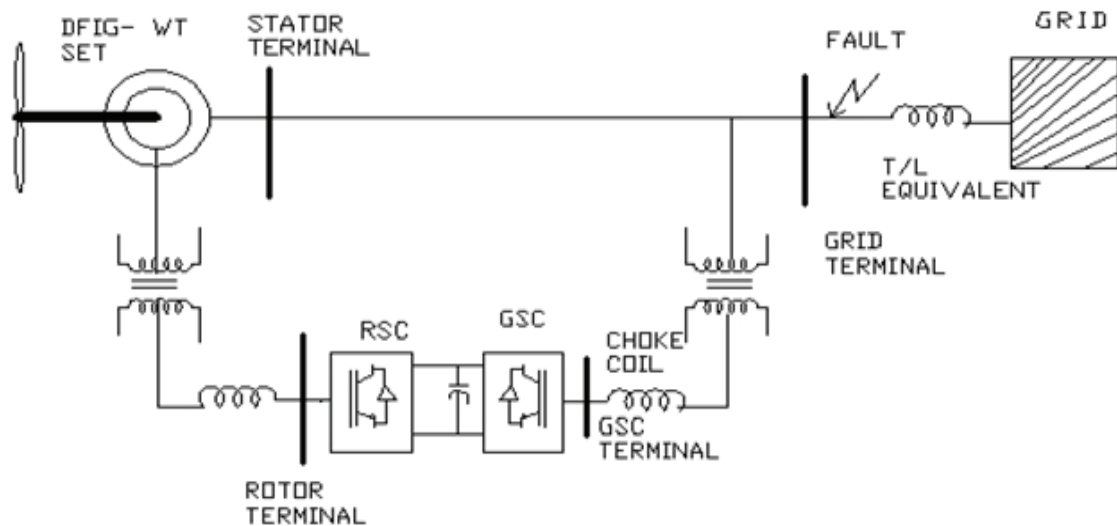

Figure 9 Design of overall DFIG based system with RSC and GSC in MATLAB/ SIMULINK
3.2 Behavior of mechanical and electrical system with the variation in wind speed and reactive power

The mechanical to electrical relationship is explained as follows. The rotor speed can be expressed as

$$\omega_r = (1-s)\omega_s = p\eta\omega_{\omega t} \tag{33}$$

Where s is slip of DFIG, p is pair of poles of DFIG; η is gear box ratio and $\omega_{\omega t}$ is wind turbine speed. With the change in wind speed and depending on gears ratio and number of field poles, the rotor speed varies is shown in equation 33. When rotor speed varies, reference quadrature axis current changes, thereby current flow in the rotor circuit varies. The stator output also varies with variation in wind turbine speed and DFIG output power. When slip varies, the voltage in rotor circuit also varies which can be explained as per equations 8 and 9. Further change in rotor voltage leads to change in rotor current, there by rotor power flow also varies.

The mechanical turbine tip speed ratio (TSR) can be written in terms of radius of turbine wings (R), angular stator speed (ω_s), pole pairs and gear box ratio as

$$\lambda = \frac{R\omega_s}{p\eta v_w}(1-s) \tag{34}$$

Increase in stator or grid frequency, TSR increases and vice versa. Similarly with increase in rotor speed or wind speed, TSR decreases and vice versa. Hence when an electrical system gets disturbed, mechanical system also will get some turbulence and electrical to mechanical system is tightly interlinked. The steady state behavior of overall system must satisfy the relation below.

$$\Delta P = \frac{-P_{\omega t}}{(1-s)} - P_{em} = 0 \tag{35}$$

Under normal conditions, the change in turbine output has to be compensated by electrical power output from DFIG. Otherwise slip gets changed and thereby rotor speed changes. Hence imbalance in mechanical to electrical power output ratios, the slip changes. With the change in coefficient of power C_p, the mechanical power varies. The mechanical power changes mostly when wind speed or air density around the turbine wings changes. The electrical power from DFIG changes when mechanical power changes or rotor speed changes or load demand from grid varies.

4. Results and Discussion

The dynamic performance of the DFIG system is shown in Fig. 9 is investigated under three different cases and the rating specifications for DFIG and wind turbine parameters are given in appendix. The wind speed change in all cases in meters per seconds as 8, 15, 20 and 10 at 15, 25 and 35 seconds. The reactive power and voltage value change in individual two cases with change in time is from -0.6pu at 12 seconds to 0pu change at 20 seconds. It was further changed from 0pu to +0.6pu magnitude at 30 seconds. In general wind speed will change with time which is a natural phenomenon, demand in lagging or leading reactive power will come into picture because of change in load. Due to addition of large furnace or induction motor or non-linear type load, leading reactive power greater than 0pu is required, while for light load lagging reactive power is required (<0pu). Hence DFIG will become better generator source if immediately it can supply any desired reactive power effectively. The change in grid terminal voltage takes place when suddenly switching on or off large loads or due to small faults near point of common coupling (PCC). The effect of change in wind speed, change in wind speed with reactive power and change in wind speed with grid terminal voltages on generator and turbine parameters are studied.

5. Case Studies

Case – A: Change in TSR and C_p with wind speed, reactive power and grid voltage
        The changes in tip- speed ratio and power coefficient C_p with change in wind speed alone is shown in Fig.10 (i), with both reactive power and wind speed variation in Fig.11 (ii) and variation with grid terminal voltage and wind speed both is shown in Fig.10 (iii). It can be observed that when wind speed is at 8m/s, tip speed ratio (TSR) is high near 4.8 degrees and slowly decreases to 2.6 degrees at 15s when speed increases to 15m/s, further increased to 1.9^o at 25s when speed of wind is 20m/s and decreased to 3.9^o when wind speed decreased to 10m/s at 35s. In the similar way, C_p is also changing from 3.25 to 1.7 at 15s, and further decreased to 1.25 at 25s, and then increased to 2.55 at 35 seconds with wind speed variation from 8 to 15 and then to 20, and 10 m/s.
        The variation in TSR and C_p with change in reactive power is independent and has no effect as shown in Fig.10 (i & ii). However, with change in grid terminal voltage, a very small change in TSR and C_p can be observed. It is due to the fact that the TSR and Cp depends on parameters as described by equations 1 to 5 and is independent on voltage and reactive power. The TSR and C_p are blade size and shape with change in ambient temperature and wind speed dependent natural parameters.

Case – B: Change in electromagnetic torque and rotor speed with wind speed, reactive power and grid voltage
        The reference mechanical turbine torque and generator torque with magnitudes overlapping and variation of rotor speed for all three cases comparison is shown in Fig 11. In this the reference and actual torque waveform with blue color is turbine reference torque and pink color lines are for generator torque. It can be observed in Fig. 11 (i, ii and iii), with increase in wind speed, torque is increasing and vice-versa. Till time up to 15 seconds, wind speed is at low value of 8m/s, so torque is at -0.2pu and increased to -0.5pu at 15s with increase in wind speed to 15m/s. The torque further increased to -0.9pu when wind speed is 20m/s and decreased to -0.28pu when speed decreased to 10m/s. there are small surges in torque waveform because of sudden change in wind speed. These surges can be minimized if a flywheel is used between turbine and generator, but has disadvantage of increase in weight, cost and maintenance. With the change in wind speed, rotor speed is also varying but is maintained nearly at constant value of 1.3pu RPM. In the first case, reactive power was at 0pu and grid terminal voltage is 1pu.
        The changes in torque has effect with change in reactive power as in Fig. 11 (ii) and further more surges been observed when grid voltage disturbance occurred as in Fig11 (iii) is taking place. When reactive power is lagging at -0.6pu, there is a small surge in torque at 20 seconds. Generator speed is also low at 1.27pu at -0.6pu reactive power, while at 0pu reactive power, it is 1.32pu speed. But rotor speed increased to 1.4pu speed at low terminal grid voltage of 0.8pu. When, reactive power changes to 0pu from -0.6pu, rotor speed increased to 1.3pu from 1.27pu and grid terminal voltage changes to 1pu from 0.8pu between 20 to 30 seconds. Speed further increased to 1.35pu with leading reactive power of +0.6pu and decreased when grid voltage increased from 1pu to 1.2pu. Therefore rotor speed increases if reactive power changes from lagging (-ve) to leading (+ve) and rotor speed decreases with increase in grid terminal voltage beyond 1pu value in rms. The surges in torque will be observed very high when terminal grid voltage changes is due to the fact of change in mechanical power is not that faster than in comparison with electrical power change, which can be understandable using equal area criterion for SMIB system.

Case – C: Change in stator voltage and current with wind speed, reactive power and grid voltage
        The change in stator voltage and current with all three cases is shown in Fig. 12 and zoomed voltage and current is shown in Fig. 13. It can be observed that the stator terminal voltage is constant with change in wind speed as in Fig. 12 (i) or with change in reactive power as in Fig. 12 (ii). There is an increase in current from 0.18pu to 0.5pu at 15 seconds with increase in wind speed from 8 to 15m/s and further increased to 0.9pu amps when speed increased to 20m/s and decreased to 0.3pu amps when speed of wind is 10m/s as shown in Fig. 12 (i). But with change in reactive power, terminal voltage is nearly constant but there is a large change in current and voltage angle, hence large

magnitude and angle change in current. When reactive power (Q) change from 0pu to -0.6pu, current increased from 0.15pu 0.5pu amps and decreased to 0.5pu amps when Q changes from -0.6pu to 0pu and increased to 1pu amps when speed of wind is 20m/s and reactive power is 0.6pu.
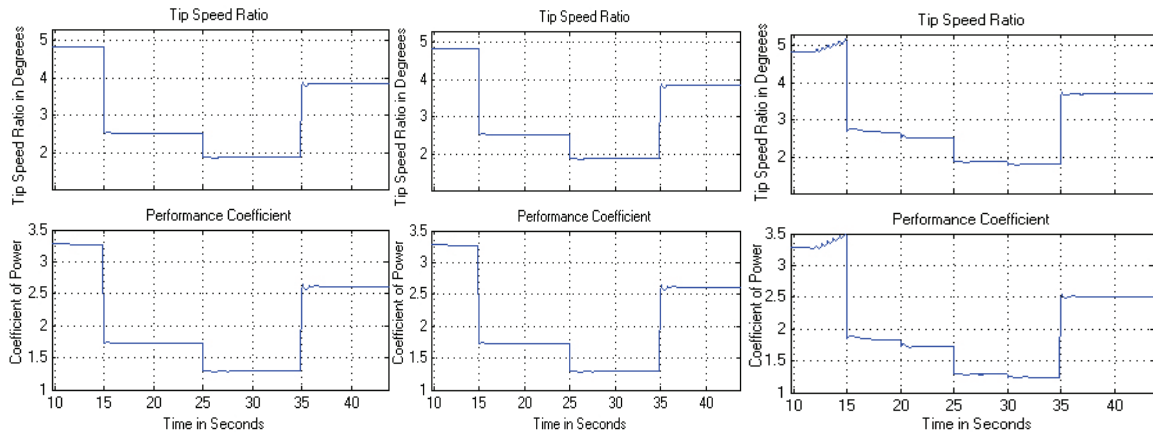

Fig. 10 (i)   Fig. 10 (ii)   Fig.10 (iii)

Figure 10 Tip speed ratio and Coefficient of power C_p for (i) change in wind speed alone, (ii) reactive power change & wind speed variation, (iii) both grid voltage & wind speed changes
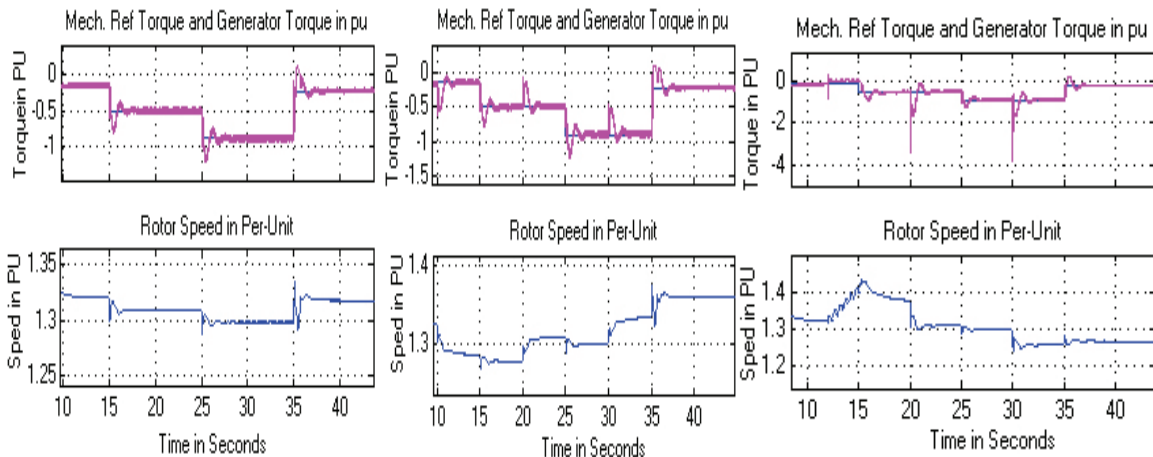

Fig. 11 (i)   Fig. 11 (ii)   Fig. 11 (iii)

Figure 11 Reference and actual generator torque and rotor speed variation with time for (i) change in wind speed alone, (ii) reactive power change & wind speed variation, (iii) both grid voltage & wind speed changes
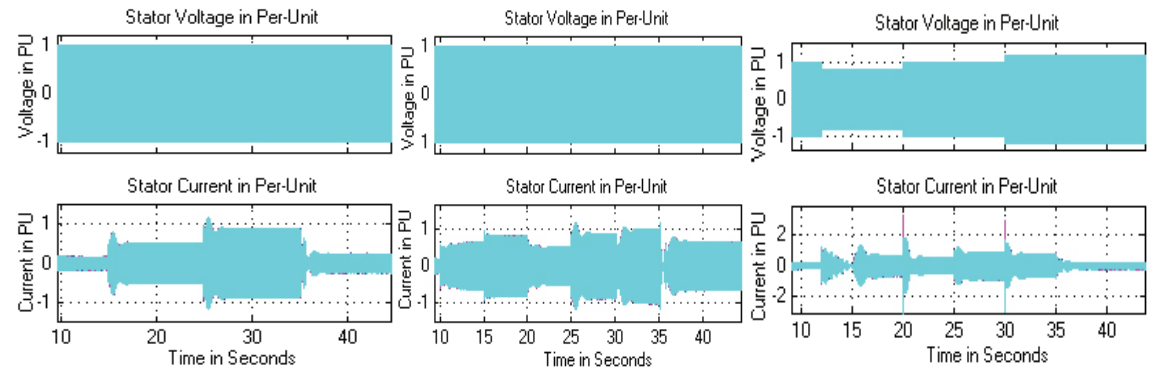

Fig. 12 (i)   Fig. 12 (ii)   Fig. 12 (iii)

Figure 12 Stator voltage and current for (i) change in wind speed alone, (ii) reactive power change & wind speed variation, (iii) both grid voltage & wind speed changes
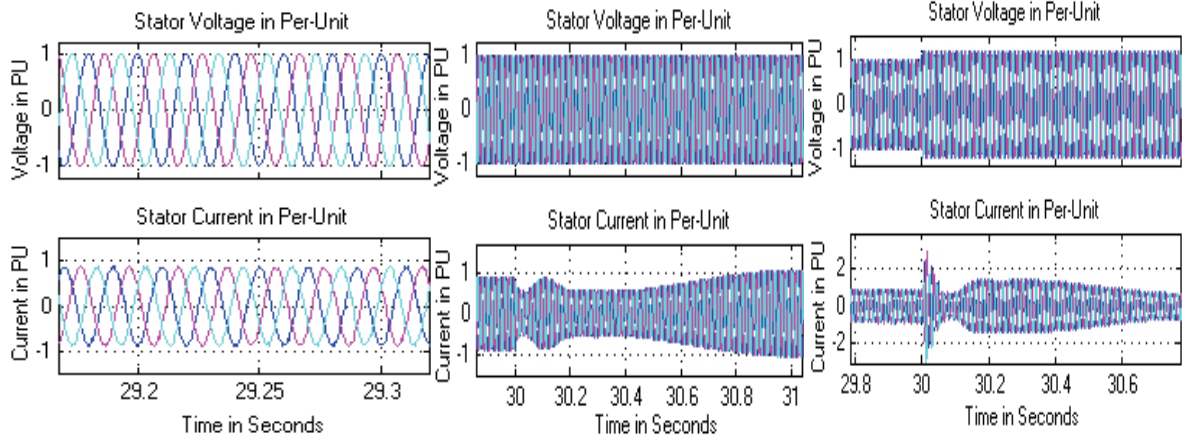
Fig. 13 (i)   Fig. 13 (ii)   Fig. 13 (iii)

Figure 13 Stator voltage and current for (i) change in wind speed alone, (ii) reactive power change & wind speed variation, (iii) both grid voltage & wind speed changes

Fig. 14 (i)   Fig. 14 (ii)   Fig. 14 (iii)

Figure 14 Rotor voltage and current (i) change in wind speed alone, (ii) reactive power change & wind speed variation, (iii) both grid voltage & wind speed changes

Fig. 15 (i)   Fig. 15 (ii)   Fig. 15 (iii)

Figure 15 Rotor voltage and current for (i) change in wind speed alone, (ii) reactive power change & wind speed variation, (iii) both grid voltage & wind speed changes
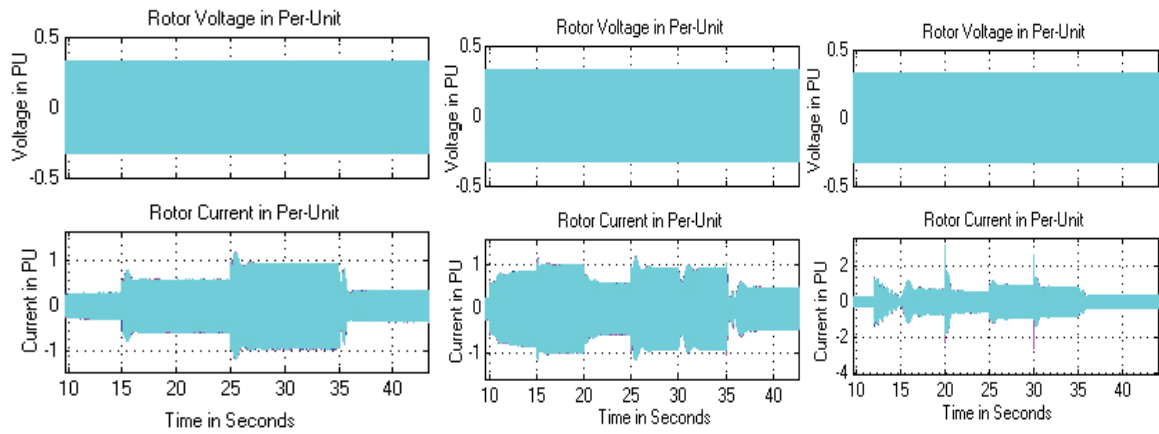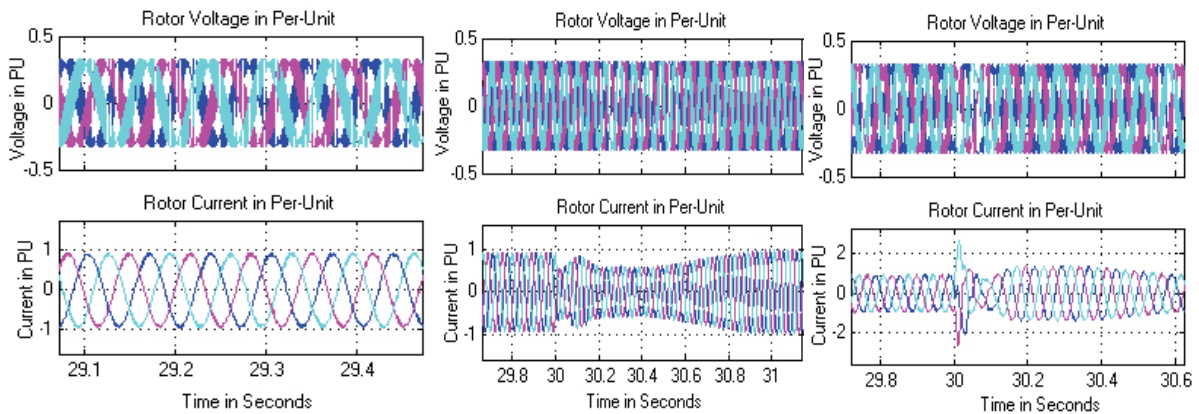
60

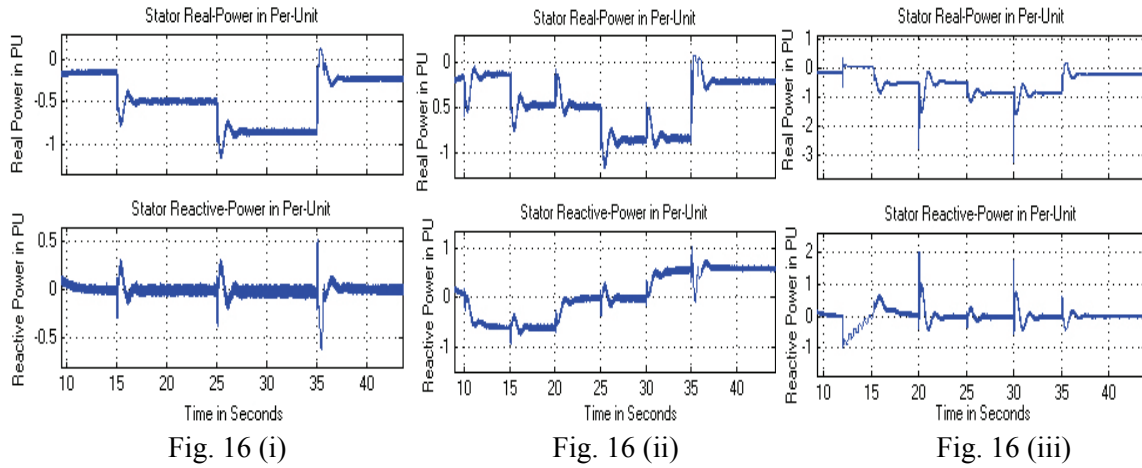Fig. 16 (i)   Fig. 16 (ii)   Fig. 16 (iii)

Figure 16 Stator real and reactive power waveform with time for (i) change in wind speed alone, (ii) reactive power change & wind speed variation, (iii) both grid voltage & wind speed changes

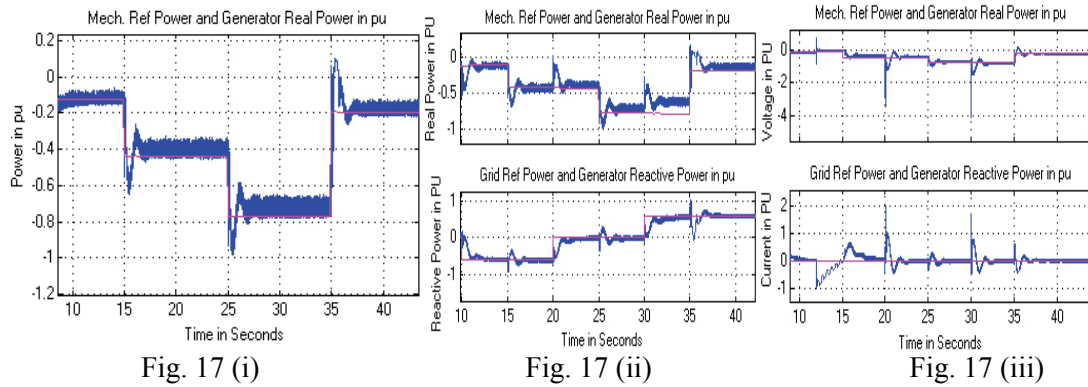Fig. 17 (i)   Fig. 17 (ii)   Fig. 17 (iii)

Figure 17 generator reference and actual real power waveform with time for (i) change in wind speed alone, generator real and reactive power flows for actual and reference for change in (ii) reactive power change & wind speed variation, (iii) both grid voltage & wind speed changes

With sudden decrease in grid terminal voltage from 1pu to 0.8pu volts at 12 seconds, slowly stator current decreased exponentially when wind speed is very low of 0.1pu amps at 8m/s and this current was improved to 1pu when wind speed increased to 15m/s. But when terminal voltage changed to 1pu from 0.8pu at 20s, current again reached to normal value of 0.5pu amps as in case 1 and the current increased to again 1pu when wind speed reaches 20m/s. when the grid terminal voltage increased to 1.2pu from 1pu, the stator current again decreased to 0.8pu amps and when wind speed finally reaches 10m/s with voltage at 1.2pu, the current is 0.2pu Amps as in Fig.12 (iii) and 12 (i). Hence with increase in voltage at constant wind speed, current decreases and with increase in wind speed at same voltage current will increase and vice-versa. The zoomed stator voltage and current waveform for a particular time period of nearly 1 second for all three cases is shown in Fig. 13. In the similar way as does in stator voltage and current, rotor voltage and current will also vary, but rotor current is bi-directional unlike stator current does.

Case – D: Change in rotor voltage and current with wind speed, reactive power and grid voltage

In all the three cases, rotor voltage is nearly constant at 0.32pu, but current is varying with variation in wind speed alone Fig. 14 (i), with both wind speed and reactive power change in Fig. 14 (ii) and for voltage and wind speed variation as in Fig 14 (iii). For the first case, with increase in rotor speed, rotor current increases and vice versa. When wind speed is at 8m/s, rotor current is 0.2pu, when wind speed reaches 15m/s, rotor current is 0.5pu, it is 0.9pu when wind speed is 20m/s and is 0.3pu when wind speed is 10m/s as shown in Fig. 14 (i) and zoomed picture in Fig. 15(i). But when reactive power at -0.6pu, rotor current is 0.8pu is even low at 8m/s wind speed and increased to 1pu amps when wind speed reaches 15m/s as in Fig. 14 (ii). When reactive power reaches 1pu, rotor

current is 0.5pu amps at wind speed of 15m/s and for leading reactive power of +0.6pu, the rotor current is again 1pu at wind speed of 20m/s and 0.5pu amps at 10m/s wind speed. With increase in wind speed or at leading or lagging reactive power, rotor current is also increasing like stator current.

In the same scenario, rotor current is decreasing with increase in grid terminal voltage and vice-versa but without any appreciable change in rotor voltage. With sudden changes in voltage at 12, 20 and 30 seconds as in Fig. 14 (iii), there are few spikes in rotor current due to sudden reversal of current magnitude and angle with respect to terminal voltages respectively. The zoom in rotor voltage and current in the time period between 29.8 to 30.6 seconds for change in voltage and wind speed is shown in Fig. 15 (iii).

Case – E: Change in stator real and reactive power with wind speed, reactive power and grid voltage
The stator real and reactive power flow for all three cases is shown in Fig. 16. The reference power which is the mechanical power output from turbine and actual generator real power change is shown in Fig. 17. In the first case with change in wind speed, with very low wind speed of 8m/s, output stator real power is 0.1pu watts till 15 seconds. When wind speed reaches 15m/s, stator real power increased to 0.5pu and further increased to 0.8pu for 20m/s wind speed at 25s and decreased to 0.2pu power at 35s for 10m/s speed as shown in Fig. 16 (i). During the change in wind speed, real power alone is changing and reactive power is constant at reference of 0pu. There are few surges in the reactive power due to change in voltage angle with respect to grid and also mainly due to change in stator and rotor current flows and rotor voltage change. With the change in reactive power demand from grid from 0pu to -0.6pu and +0.6pu at 12 and 30 seconds are shown in Fig.16 (ii). It can be observed that with change in reactive power from 0pu to -0.6pu, reactive power from generator is changing with a small time lag of 0.8s and real power maintained nearly constant value of 0.1pu at 8m/s wind speed. Similarly with reactive power changing to 0pu and +0.6pu, the reactive power is changing within 1 second and real power is almost constant with small surges in real stator power during this transient.

In third case with both voltage and wind speed changing, with the grid voltage variation from 1 to 0.8pu at 12th second, real power which is at 0.1pu changed to 0.05pu and reactive power which is at 0pu reached 1pu at this 12th second instant and slowly decaying to reach to reference 0pu value. This change in reactive power is to make voltage of stator to get adjusted to grid voltage without losing synchronism. Similarly when grid voltage reached to 1pu standard value at 20th second,

Case – F: Comparison of reference and actual stator real and reactive power with change in wind speed, reactive power and grid voltage
The reference mechanical power output is shown with pink line and generator power is with blue line for the first case is shown in Fig. 17 (i). It can be observed that, nearly generator actual power is matching with reference power and the mismatch is because of losses in turbine, gear wheels and generator and this mismatch is inevitable. With increase in wind speed, reference power is increasing and vice versa. When wind speed is 8m.s, output electrical real power is 0.1pu till 15s and reaches 0.4 and 0.8pu at 15 and 25 seconds with wind speed changing from 15 to 25m/s and then decreases to 0.2pu due to decrease in wind speed to 10m/s respectively. With the change in voltage at grid, stator terminal real power is maintained at constant value but with surges at instant of transient but reactive power is adjusting till stator voltage reaches the grid voltage for maintaining synchronism as shown in Fig. 16 (iii) and 17 (iii). At the instant of 20 and 30 seconds, there is surge in real and reactive powers but were maintaining constant stator output real powers of 0.5 and 0.8pu watts and 0pu Var as in Fig. 16 (iii).

The Figure 16 is the output real and reactive powers from stator and rotor adding vector ally as shown in blue color lines and reference real power from turbine and reactive power from grid terminal in pink. To meet the desired grid reactive power, both stator and rotor has to supply for faster dynamics with an aid to RSC and GSC control schemes and is achieving as shown in Fig. 17 (ii). With the change in wind speed and reactive power, real power from generator is matching its reference value for case 2, but small deviation can be observed from time 30 to 35 seconds is due to sudden change in reactive power demand from grid and the deviation in real power is from 0.8pu to 0.7pu which is small. However reactive power is following its trajectory within 1 second.

In the case 3, both voltage and reactive power changing with time, total output real and reactive powers from stator and rotor is delivering to grid to meet the desired grid power demand. Unlike with change in reactive power, change in voltage is not affecting any deviation in real power and is following the trajectory nearly accurate with maximum deviation of 5% in real power. The reactive power change with grid voltage is high when voltage decreased from 1pu to 0.8pu volts.

When wind speed is increasing, mechanical and electrical torques are increasing without any change in stator reactive power. Variation in grid reactive power causes quadrature currents on both stator and rotor to change but torque, speed or real powers from stator or rotor remains unaltered. The variation in grid terminal voltage, a very small change in TSR and C_p can be observed. It is due to the fact that the TSR and C_p depends on parameters and is independent on voltage and reactive power. The TSR and C_p are blade size and shape with change in ambient temperature and wind speed dependent natural parameters. With increase in voltage at constant wind speed, current decreases but, with increase in wind speed at same voltage, current will increase and the decrease in wind speed caused current from stator to rotor decreases with stator voltage as constant as depicted by grid. In the similar way as does in stator voltage and current, rotor voltage and current will also vary, but rotor current is bi-directional unlike stator current. The change in voltage at grid, stator terminal real power is maintained at constant value but with surges at instant of transient but reactive power is adjusting till stator voltage reaches the grid voltage for maintaining synchronism. To meet the desired grid reactive power, both stator and rotor has to supply for faster dynamics and it depends on faster action of RSC and GSC control schemes. The change in three cases is tabulated below. The variation in reactive power and grid voltage variations during the respective time period is shown in Table 2 and Table 3. In the Table 1, due to change in wind speed input to turbine alone, generator and wind turbine parameters changes are summarized. There are surges produced in electromagnetic torque (EMT) due to variations in reactive power and grid voltage. Large spikes in stator current and rotor current are produced due to sudden increase or decrease in grid voltage. Certain deviations in rotor speed can be observed due to change in reactive power or grid voltage. It is due to variation in current flow in the rotor circuit, thereby variation in rotor flux and hence rotor speed.

Table 1: Change in Reactive power during the time period along with change in wind speed

Time range (s)	0.-20	20-30	30-50
Reactive power (pu)	-0.6	0	0.6

Table 2 Change in grid voltage during the time period along with change in wind speed

Time range (s)	0.-12	12-20	20-30	30-50
Reactive power (pu)	1	0.8	1	1.2

Table 3 Variation of turbine and generator parameters with change in wind speed input

Wind speed (m.s)	8	15	20	10
Time (s)	10	15	25	35
TSR (degree)	4.9	2.5	1.95	3.95
Cp	3.25	1.75	1.25	2.60
EMT (pu)	-0.2	-0.5	-0.8	-0.3
Rotor speed (pu)	1.32	1.31	1.30	1.33
Stator current (pu)	0.2	0.5	0.8	0.3
Rotor current (pu)	0.25	0.55	0.90	0.35
Stator power (pu)	-0.2	-0.5	-0.8	-0.3
Rotor power (pu)	0	0	0	0

6. Conclusion

From the proposed control scheme, the torque, speed and reactive power control of DFIG is very precise. With change in wind speed, electromagnetic torque surges are low and the variation in wind speed is not getting the generator rotor speed altered due to better transition in gear wheel mechanism. Reactive power demand from grid is accurate which can be met by proper control action of RSC and GSC. The proposed methodology is accurate and following all basic mathematical equations explained in previous section. Distinct from reactive power variation, change in voltage is not affecting any deviation in real power and is following the trajectory nearly accurate with maximum deviation of 5% in real power. The reactive power change with grid voltage is high when voltage decreased from 1pu to 0.8pu volts. Hence the proposed control scheme can be applied with ever changing transients like large variation in wind speed, reactive power and grid voltage. The system is very stable without loosing synchronism when grid voltage is increasing or decreasing to a ±0.2pu change from nominal voltage value.

Appendix

The parameters of DFIG used in simulation are,
Rated Power = 1.5MW, Rated Voltage = 690V, Stator Resistance Rs = 0.0049pu, rotor Resistance Rr = 0.0049pu, Stator Leakage Inductance Lls = 0.093pu, Rotor Leakage inductance Llr1 = 0.1pu, Inertia constant = 4.54pu, Number of poles = 4, Mutual Inductance Lm = 3.39 pu, DC link Voltage = 415V, Dc link capacitance = 0.2F, Wind speed = 14 m/sec.
Grid Voltage = 25 KV, Grid frequency = 60 Hz.
Grid side Filter: Rfg = 0.3Ω, Lfg = 0.6nH
Rotor side filter: Rfr = 0.3mΩ, Lfr = 0.6nH
Wind speed variations: 8, 15, 20 and 10 at 15, 25 and 35 seconds.
Reactive power change: -0.6 to 0 and +0.6pu at 20 and 30 seconds.
Grid voltage change: 0.8 to 1 and to 1.2pu at 20 and 30 seconds.

References

[1]   Aghanoori, N, Mohseni, M, Masoum, M.A.S, "Fuzzy approach for reactive power control of DFIG-based wind turbines", IEEE PES Innovative Smart Grid Technologies Asia (ISGT), 2011, pp: 1-6

[2]   Syed Muhammad Raza Kazmi, Hiroki Goto, , Hai-Jiao Guo, Osamu Ichinokura, "A Novel Algorithm for Fast and Efficient Speed-Sensor less Maximum Power Point Tracking in Wind Energy Conversion Systems", IEEE Transactions On Industrial Electronics, Vol. 58, No. 1, January 2011, pp: 29-36

[3]   Iwanski, G, Koczara, W, "DFIG-Based Power Generation System With UPS Function for Variable-Speed Applications", IEEE Transactions on Industrial Electronics, Vol: 55, No. 8, Aug. 2008, pp: 3047 – 3054

[4]   Aktarujjaman, M.; Haque, M.E; Muttaqi, K.M. Negnevitsky, M., Ledwich, G, "Control Dynamics of a doubly fed induction generator under sub- and super-synchronous modes of operation", IEEE Power and Energy Society General Meeting - Conversion and Delivery of Electrical Energy in the 21st Century, 2008, pp: 1 – 9

[5]   Iwanski, G., Koczara, W., "DFIG-Based Power Generation System With UPS Function for Variable-Speed Applications", IEEE Transactions on Industrial Electronics, Vol:55, No: 8, Aug. 2008, pp: 3047 - 3054

[6]   Dawei Zhi ; Lie Xu, "Direct Power Control of DFIG With Constant Switching Frequency and Improved Transient Performance", Ieee Transactions On Energy Conversion, Vol. 22, No. 1, March 2007, pp: 110 – 118

[7]   Lie Xu ; Cartwright, P;, "Direct active and reactive power control of DFIG for wind energy generation", IEEE Transactions on Energy Conversion, , Vol. 25, No. 4, Dec 2010, pp: 1028-1039

[8]   Mustafa Kayıkc ,ı and Jovica V. Milanovi´;, "Reactive Power Control Strategies for DFIG-Based Plants", IEEE Transactions On Energy Conversion, Vol. 22, No. 2, June 2007, pp: 389-396

[9]   Stephan Engelhardt, Istvan Erlich, Christian Feltes, Jorg Kretschmann, Fekadu Shewarega, "Reactive Power Capability of Wind Turbines Based on Doubly Fed Induction Generators", IEEE Transactions On Energy Conversion, Vol. 26, No. 1, March 2011, pp: 364- 372

[10]   Gerardo Tapia, Arantxa Tapia, and J. Xabier Ostolaza, "Proportional–Integral Regulator-Based Approach to Wind Farm Reactive Power Management for Secondary Voltage Control", IEEE Transactions On Energy Conversion, Vol. 22, No. 2, June 2007, pp: 488- 498

[11]   Dongkyoung Chwa and Kyo-Beum Lee, "Variable Structure Control of the Active and Reactive Powers for a DFIG in Wind Turbines", IEEE Transactions On Industry Applications, Vol. 46, No. 6, November/December 2010, pp: 2545-2555

[12]   Lingling Fan, Haiping Yin, Zhixin Miao, "On Active/Reactive Power Modulation of DFIG-Based Wind Generation for Interarea Oscillation Damping", IEEE Transactions On Energy Conversion, Vol. 26, No. 2, June 2011, pp: 513-521

[13]   Hua Geng, Cong Liu, Geng Yang, "LVRT Capability of DFIG-Based WECS Under Asymmetrical Grid Fault Condition", IEEE Transactions On Industrial Electronics, Vol. 60, No. 6, June 2013, pp: 2495-2509

[14]   Shukla, R.D.; Tripathi, R.K., "Low voltage ride through (LVRT) ability of DFIG based wind energy conversion system II", Students Conference on Engineering and Systems (SCES), 2012, Page(s): 1 - 6

[15]   Guzmán Díaz, "Optimal primary reserve in DFIGs for frequency support", International journal of Electrical Power and Energy Systems Vol: 43, 2012, pp: 1193–1195

[16]   F. Poitiers, T. Bouaouiche, M. Machmoum, "Advanced control of a doubly-fed induction generator for wind energy conversion", Electric Power Systems Research, Vol: 79, Feb 2009, pp: 1085–1096.